PCCP

The Mesodyn simulation of pluronic water mixtures using the 'equivalent chain' method

Youyong Li, Tingjun Hou, Senli Guo, Kaixuan Wang and Xiaojie Xu*

College of Chemistry and Molecular Engineering, Peking University, Beijing, 100871, P.R. China

Received 14th March 2000, Accepted 26th April 2000
Published on the Web 25th May 2000

The new dynamic density functional method—mesoscopic dynamics (Mesodyn)—was used to simulate microphage separation kinetics of aqueous pluronic solutions. The 'equivalent chain' method was used to perform the parameterization of the Gaussian chain. Three kinds of pluronic solutions, *i.e.* $(EO)_6(PO)_{34}(EO)_6$ (L62), $(EO)_{13}(PO)_{30}(EO)_{13}$ (L64) and $(EO)_{37}(PO)_{58}(EO)_{37}$ (P105), were investigated at different temperatures. The factors influencing the self-assembly morphology of the copolymer solution were discussed. The simulation results show that the less hydrophobic PO component, the less possibility there is of forming a core of the hydrophobic region. The simulation results also indicate that an increase of temperature results in a decrease in the interfacial area and an increase in the periodicity of the pluronic water system. The dynamic evolution process of the system and the factors affecting the process were also investigated and discussed here. The simulation results show that when the temperature increases, the phase separation process becomes slow.

Introduction

Many systems of academic and industrial interest are examples of soft condensed matter. These systems are composed of mesoscale structures of size 10 to 100 nm which can be found for example in polymer blends, block-copolymer systems, surfactant aggregates in detergent materials (*e.g.* shampoo), latex particles, or drug delivery systems.

In the microscopic region, the phase behavior can be modeled using a detailed molecular description, often with techniques such as molecular dynamics and Monte Carlo simulations. In the macroscopic region, phase separation models can be based on equations of state, which are fitted to macroscopic phase diagrams. In the mesoscopic region, local concentration fields can be used as collective variables, in order to obtain a description of self-assembly structures. The mesoscopic dynamics models are receiving increased attention as they form a bridge between fast molecular kinetics and slow thermodynamic relaxation of macroscale properties.

Pluronic [block PEO–PPO–PEO copolymer, PEO = poly(ethylene oxide), PPO = poly(propylene oxide)]: one type of non-ionic surfactant, is widely used in detergency, foam formation, dispersion stabilization, lubrication and drug delivery and has received wide attention in the literature.[1–5] The action of pluronic depends strongly on system morphology, which is known to include micelles that can reversibly gel, as well as bicontinuous, hexagonal and lamellar phases. There are several factors contributing to the morphology formation including temperature, polymer concentration, the length ratio of the three blocks, *etc.* The Mesodyn method was used here to simulate pluronic aqueous solutions and to study the influence of temperature, the impact of the relative block size of the polymer surfactant solution and the dynamic evolution of pluronic water mixtures.

In contrast to previous approaches aimed at classifying morphologies by means of equilibrium theories, the Mesodyn method recognizes the fact that by their very nature these patterns are irregular, and hence can only be characterized *via* the dynamic properties of the systems. From an industrial perspective this approach is much more realistic, since typical processing times are orders of magnitude shorter than the thermodynamic relaxation time, and thus such non-perfect states contribute substantially to the behavior of the final material.

Method

In the Mesodyn method, the molecules are defined on a coarse-grained level as 'Gaussian chains of beads'. Each bead is of a certain component type representing covalently bonded groups of atoms such as those given by one or a few monomers of a polymer chain. Chemically specific information about the molecular ensemble enters into Mesodyn *via* material parameters such as the self-diffusion coefficients of the bead components, the Flory–Huggins interaction parameters, the bead sizes and the molecular architecture (chain length, branching, *etc.*).

The dynamics of the system is described by a set of so-called functional Langevin equations. In simple terms these are diffusion equations in the component densities which take account of the noise in the system. By means of numerical inversions, the evolution of the component densities is simulated, starting from an initially homogeneous mixture in a cube of typical size 100–1000 nm and with periodic boundary conditions.

The basic idea in the Mesodyn method is the density functional theory. It is based on the idea that the free energy F of an inhomogeneous liquid is a functional of the local density function ρ. From the free energy, all thermodynamic functions can be derived, so that for instance phase transitions can be investigated as a functional of the density distribution in the system.

In Mesodyn, the method used to model the time evolution of a mesoscopic system is the time-dependent Ginzburg–Landau model. Ginzburg–Landau models generally consist of a phenomenological expansion of the free energy in the density, which is used to model thermodynamic forces, and a set of stochastic diffusion or modified Navier–Stokes equations to predict the time evolution. The numerical calculation involves integration of functional Langevin equations, given

an implicit inverse Gaussian density functional expression for the intrinsic chemical potentials. Local non-ideal interactions are included *via* a mean field. Mesoscopic fluctuations are introduced by the explicit inclusion of noise sources, according to the fluctuation–dissipation theorem. Work on coarse-grained time-dependent Ginzburg–Landau models can be found in refs. 6–10. For a detailed description of the theory of Mesodyn, see ref. 11.

Mesodyn is based on a dynamic variant of mean-field density functional theory. The latter is based on a theorem which basically states that there is a one-to-one mapping between the distribution functions of the system, the densities and an external potential field.

On a coarse-grained time scale, $\rho_I^0(r)$ is defined as a collective concentration field of the beads of type I at an instant of time and serves as a reference level. There will be a certain distribution of bead positions, defined as $\Psi(R_{11}, \ldots, R_{nN})$, where $R_{\delta s}$ is the position of bead s from chain δ. Given the distribution Ψ we can define the collective concentration of the beads s from all chains by the average of a microscopic density operator:

$$\rho_I[\Psi](r) \equiv \sum_{\gamma=1}^{n} \sum_{s=1}^{N} \delta_{Is}^{\mathrm{K}} \,\mathrm{Tr}\, \Psi\, \delta(r - R_{\gamma s}) \tag{1}$$

where δ_{Is}^{K} is a Kronecker delta function with value 1 when bead s is of type I and 0 otherwise. It is assumed that in the slowly relaxing liquid the interactions do not depend on the momenta and therefore the integration over coordinate space can be simplified as follows:

$$\mathrm{Tr}(O) \equiv \frac{1}{n!\Lambda^{3nN}} \int_{V^{nN}} (O) \prod_{\gamma=1}^{n} \prod_{s=1}^{N} \mathrm{d}R_{\gamma s} \tag{2}$$

where $n!$ accounts for the indistinguishability of the chains and Λ is a thermal wavelength

$$\Lambda = (h^2\beta/2\pi m)^{1/2} \tag{3}$$

and m is the mass of a bead.[12] Λ^{3nN} is the normalization coefficient which ensures that distribution Ψ is dimensionless.

We can define a set of distribution functions Ψ with the constraint that $\rho_I[\Psi](r) = \rho_I^0(r)$:

$$\Omega = \{\Psi(R_{11}, \ldots, R_{nN}) \,|\, \rho_I[\Psi](r) = \rho_I^0(r)\} \tag{4}$$

All distributions Ψ of the set Ω lead to the same density $\rho_I^0(r)$. On this set of distribution functions an intrinsic free energy functional $F[\Psi]$ can be defined:

$$F[\Psi] = \mathrm{Tr}(\Psi H^{\mathrm{id}} + \beta^{-1}\Psi \ln \Psi) + F^{\mathrm{nid}}[\rho^0] \tag{5}$$

The first term is the average value of the Hamiltonian for internal Gaussian chain interaction:[13,14]

$$H^{\mathrm{id}} = \sum_{\gamma=1}^{n} H_{\gamma}^{\mathrm{G}} \tag{6}$$

where H_{γ}^{G} is the Gaussian chain Hamiltonian of chain γ,

$$\beta H_{\gamma}^{\mathrm{G}} = \frac{3}{2\alpha^2} \sum_{s=2}^{N} (R_{\gamma s} - R_{\gamma, s-1})^2 \tag{7}$$

The coefficient α is the Gaussian bond length parameter. The second term in the free energy functional represents the Gibbs entropy of the distribution, $-k_{\mathrm{B}}T\Psi \ln \Psi$. The third term $F^{\mathrm{nid}}[\rho^0]$ is the mean-field non-ideal contribution.

The key rudiment of dynamic density functional theory is now that on a coarse-grained time scale the distribution function Ψ is such that the free energy functional $F[\Psi]$ is minimized. Hence Ψ is independent of the history of the system, and is fully characterized by the constraints that it represents the density distribution and minimizes the free energy functional. This constraint on the density fields is realized by means of an external potential U_I.

The constraint minimization of the free energy functional leads to an optimal distribution, which in turn, and by the one-to-one relation between densities, distributions and external potential, can be written as:

$$\beta F[\rho] = n \ln \Phi + \beta^{-1} \ln n! - \sum_I \int U_I(r)\rho_I(r)\, \mathrm{d}r + \beta F^{\mathrm{nid}}[\rho] \tag{8}$$

Finally, a Flory–Huggins type interaction is introduced for the non-ideal (inter-chain) interactions:

$$\begin{aligned} F^{\mathrm{nid}}[\rho] = \frac{1}{2} \int\int [&\varepsilon_{\mathrm{AA}}(|r - r'|)\rho_{\mathrm{A}}(r)\rho_{\mathrm{A}}(r') \\ &+ \varepsilon_{\mathrm{AB}}(|r - r'|)\rho_{\mathrm{A}}(r)\rho_{\mathrm{B}}(r') \\ &+ \varepsilon_{\mathrm{BA}}(|r - r'|)\rho_{\mathrm{B}}(r)\rho_{\mathrm{A}}(r') \\ &+ \varepsilon_{\mathrm{BB}}(|r - r'|)\rho_{\mathrm{B}}(r)\rho_{\mathrm{B}}(r')]\, \mathrm{d}r\, \mathrm{d}r' \end{aligned} \tag{9}$$

where $\varepsilon_{IJ}(|r - r'|)$ is a mean-field energetic interaction between beads of type I at r and J at r', defined by the same Gaussian kernel as in the ideal chain Hamiltonian

$$\varepsilon_{IJ}(|r - r'|) \equiv \varepsilon_{IJ}^0 \left(\frac{3}{2\pi\alpha^2}\right)^{3/2} \exp\left[-\frac{3}{2\alpha^2}(r - r')\right] \tag{10}$$

The mean-field intrinsic chemical potentials can easily be derived by functional differentiation of the free energy: $\mu_I(r) = \delta F/\delta\rho_I(r)$. At equilibrium $\mu_I(r) = \mathrm{const}$, which results in the familiar self-consistent field equations for the mean-field Gaussian chain model. In general, these equations will have many solutions, one of which will be a state of lowest free energy; most states will be metastable. When the system is not in equilibrium, $-\nabla\mu_I(r)$ is a thermodynamic force, which by the inversion of the density functional and the explicit form of the non-ideal interactions is a unique functional of the density. Based on these equations, we can set up a generalized time-dependent Ginzburg–Landau theory.

The derivation of the diffusive dynamics of the molecular ensemble is based on the assumption that for each type of bead I the local flux is proportional to the local bead concentration and the local thermodynamic driving force: $J_I = -M\rho_I\nabla\mu_I + J_I'$, where J_I' is a stochastic flux (related to thermal noise). Together with the continuity equation:

$$\frac{\partial\rho_I}{\partial t} + \nabla \cdot J_I = 0 \tag{11}$$

this leads to simple diagonal functional Langevin equations (stochastic diffusion equations) in the density fields with a Gaussian distribution of the noise:

$$\frac{\partial\rho_I}{\partial t} = M\nabla \cdot \rho_I\nabla\mu_I + \eta_I \tag{12}$$

However, the fluctuations in the total density of this simple system are not realistic since finite compressibility is not enforced by the mean-field potential chosen (see below). Therefore, total density fluctuations are simply removed by introducing an incompressibility constraint:

$$[\rho_{\mathrm{A}}(\boldsymbol{r}, t) + \rho_{\mathrm{B}}(\boldsymbol{r}, t)] = \frac{1}{v_{\mathrm{B}}} \tag{13}$$

where v_{B} is the average bead volume. This condition then leads to 'exchange' Langevin equations:

$$\frac{\partial\rho_{\mathrm{A}}}{\partial t} = Mv_{\mathrm{B}}\nabla \cdot \rho_{\mathrm{A}}\rho_{\mathrm{B}}\nabla[\mu_{\mathrm{A}} - \mu_{\mathrm{B}}] + \eta \tag{14}$$

$$\frac{\partial\rho_{\mathrm{B}}}{\partial t} = Mv_{\mathrm{B}}\nabla \cdot \rho_{\mathrm{A}}\rho_{\mathrm{B}}\nabla[\mu_{\mathrm{B}} - \mu_{\mathrm{A}}] - \eta \tag{15}$$

Here M is a bead mobility parameter. The kinetic coefficient $Mv\rho_A\rho_B$ models a local exchange mechanism. Hence the model is strictly valid only for Rouse dynamics.

The distribution of the Gaussian noise satisfies the fluctuation–dissipation theorem and ensures that the time integration of the Langevin equations generates an ensemble of density fields with Boltzmann distributions:

$$\langle \eta(r, t)\rangle = 0 \tag{16}$$

$$\langle \eta(r, t)\eta(r', t')\rangle = -\frac{2Mv_B}{\beta}\,\delta(t - t')\nabla_r \times \delta(r - r')\rho_A\rho_B\nabla_{r'} \tag{17}$$

Results and discussion

The phase separation kinetics and phase structure of pluronic water mixtures have been studied for three poly(ethylene oxide)-*b*-poly(propylene oxide)-*b*-poly(ethylene oxide) (PEO–PPO–PEO) block copolymers of different compositions, $(EO)_6(PO)_{34}(EO)_6$ (L62), $(EO)_{13}(PO)_{30}(EO)_{13}$ (L64) and $(EO)_{37}(PO)_{58}(EO)_{37}$ (P105), by using the Mesodyn simulation method. Temperature is discussed here as an influencing factor. The time evolution trajectory of the microphage separation kinetics is also discussed in detail.

The 'equivalent chain'[12] method was used to find a Gaussian chain which behaves as the pluronic molecule. In this method, the Gaussian chain parameters N and α are calculated from the end distribution $\langle r^2\rangle$ and the length along the chain Σl_i (l_i is the length of backbone bond i).

The end distribution for the $(EO)_X(PO)_Y(EO)_X$ molecule can be estimated from the characteristic ratios as

$$\langle r^2\rangle = 2XC_\infty^{EO}(l_{CC}^2 + 2l_{CO}^2) + YC_\infty^{PO}(l_{CC}^2 + 2l_{CO}^2) \tag{18}$$

and the length of the backbone is

$$\sum l_i = (2X + Y)(l_{CC} + 2l_{CO}) \tag{19}$$

Table 1 shows the parameters used here for the $(EO)_X(PO)_Y(EO)_X$ molecule. The characteristic ratios for EO and PO homopolymers used here are 5.2[13] and 6.0[14] respectively. These values are determined by experiments.

Table 1 The parameters for the $(EO)_X(PO)_Y(EO)_X$ molecule

L_{CC}	0.153 nm
L_{CO}	0.143 nm
$L_{CC} + 2L_{CO}$	0.439 nm
$L_{CC}^2 + 2L_{CO}^2$	0.0646 nm^2
C_∞^{EO}	5.2
C_∞^{PO}	6.0

Table 2 The Gaussian chain parameters

Polymer	Molecular formula	Gaussian chain	N	α/nm
L62	E6P34E6	E3P18E3	24	0.84
L64	E13P30E13	E7P16E7	30	0.82
P105	E37P58E37	E20P31E20	71	0.82

For a Gaussian chain $\langle r^2\rangle = N\alpha^2$ and $\Sigma l_i = N\alpha$, which, combined with eqns. (18) and (19), can give the results of the Gaussian chain parameters. Table 2 shows the results.

The solvent–polymer interaction parameters were calculated from vapor pressure data of aqueous homopolymer solutions,[11] using the Flory–Huggins expression

$$\chi_{IJ} = \theta^{-2}\{\ln(p/p^0) - \ln(1 - \theta) - (1 - 1/N')\theta\} \tag{20}$$

where p is the vapor pressure and θ is the polymer volume fraction. The parameter N' is the chain length, which was the number of monomers per bead. Table 3 shows the value of N' for L62, L64 and P105 respectively. The results indicate that all N' are nearly equal to 2, and so we used 2 as the value of N' to perform the parameterization. The polymer volume fraction θ in our simulations is the same value: 0.50. So the interaction parameters used here are $\chi_{ES} = 1.4$, $\chi_{PS} = 1.7$ for all the calculations. The parameter χ_{EP} used was the estimated value 4.0.

The mesoscopic dynamics simulations were performed by using the Mesodyn module of Cerious2. The dimensions of the simulation lattice used here are (32, 32, 32). The ratio of the bond length α and the cell length h is automatically set to $\alpha/h = 1.15430$ to ensure isotropy of all grid-restricted operators.[15]

The bead volume v of three types E, P, S used here was 300 Å^3 and the bead diffusion coefficients $D = \beta^{-1}M$ of three types were set at 1.0×10^{-7} cm^2 s^{-1}.

The product of the time step and the diffusion coefficient affects the actual dimensionless time step taken by the program. To ensure a stable numerical algorithm, it is advisable to choose all diffusion coefficients D and time step such that their product divided by the cell size squared is between 0.1 and 1.0. The time step used here was 50.00 ns.

Table 3 The value of N' for L62, L64 and P105

	L62	L64	P105
E	6/3	13/7	37/20
P	34/18	30/16	58/31

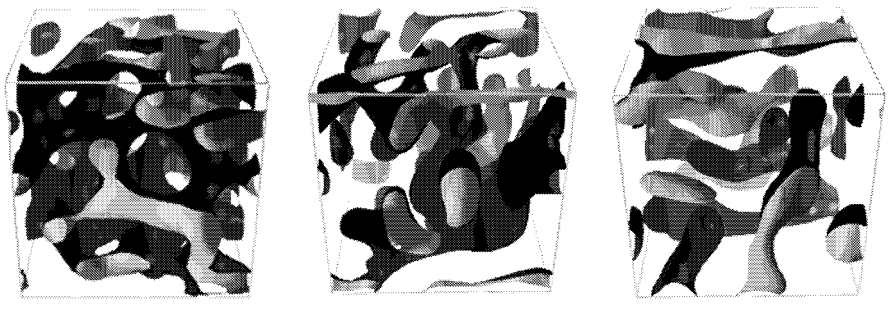

(a) (b) (c)

Fig. 1 PO isosurface representations of the (a) L62, (b) L64, and (c) P105 solutions.

The noise scaling parameter used was 100 and the compressibility parameter was fixed at 10.0 (see refs. 16 and 17 for detailed discussion).

To compare the three types of pluronic water mixture, the simulations were performed with the same polymer concentration. Volume concentration in all cases was 0.50 here. Fig. 1 shows the morphology of the systems of different copolymers after 1000 simulation steps. The figure shows the isosurface of bead PO at isolevel $\theta_{PO} = 0.70$. The simulation temperature was set at 298 K here.

The simulation result shows that the L62 solution forms a gel morphology. The morphology of L64 solutions is a transition between gel and micelle. The P105 solution forms a micelle morphology. This is in agreement with experimental results.[18]

Although the molecular weight of the polymers is in the order L62 < L64 < P105, the content of the PO component is in the opposite order P105 < L64 < L62. The less hydrophobic PO component, the less possibility there is of forming a core of the hydrophobic region. In this respect the result is reasonable.

Several simulations have been performed to discuss the effects of temperature on the phase behavior of the copolymers. The three pluronic water mixtures have been simulated at three different temperatures: 298 K, 323 K, 373 K. Figs. 2–4 show the Fourier transform result of the density field of L62 solution (volume concentration was 0.50) after 1000 steps of the Mesodyn simulation.

The primary peaks of the three figures are located at 0.142, 0.154, 0.176 respectively. This means that, with the increase of the temperature, the periodicity of the density field shifts from 7.04 Å, 6.49 Å to 5.68 Å. The Fourier transform results indicate that, with the increase of the temperature, the frequency of the density field increases too. This is in agreement with Alexandridis's experimental results.[18] An increase of the temperature results in a decrease in the interfacial area and an increase in the periodicity of the L62–water system. Brown's experimental work[19] gives a similar conclusion that the apparent micellar radius decreases with increasing temperature.

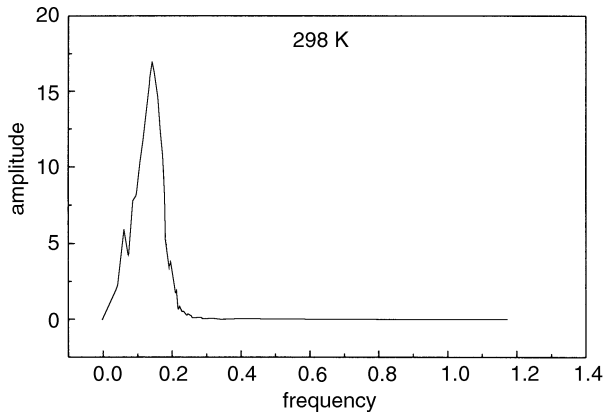

Fig. 2 The Fourier transform of the density field of L62 solution at 298 K.

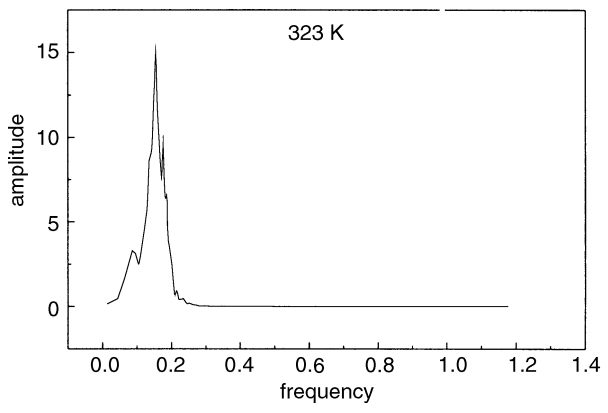

Fig. 3 The Fourier transform of the density field of L62 solution at 323 K.

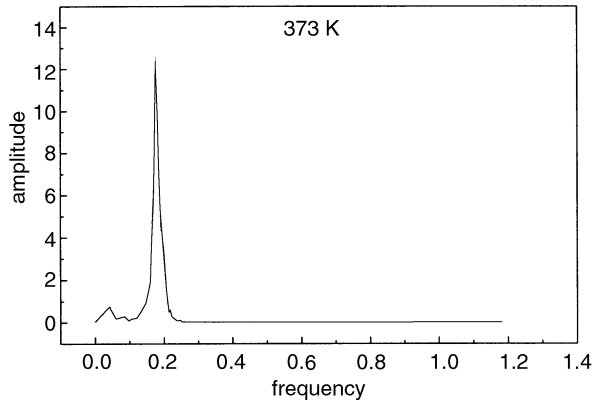

Fig. 4 The Fourier transform of the density field of L62 solution at 373 K.

Till now, there has been no experimental information about the time scale of the phase separation of the pluronic water mixture. The microphage structures are determined after days or weeks of equilibrium time, while the phase separation kinetics is artificially enhanced by repeated centrifugation.[20]

The Mesodyn simulation clearly gives the phase separation process. Fig. 5 gives the time evolution of the order parameter P of L62 solution simulated at 298 K. The dimensionless order parameter P is defined as $P = V^{-1} \Sigma \int \theta_I^2(r)\, dr - \Sigma(\theta_I^0)^2$.

Fig. 5 shows that the time evolution of the phase separation can be divided into two stages. First, the system rapidly formed the raw morphology of micelle or gel. In this stage, the order parameter ascended quickly. The first stage takes 10 μs. Second, the system changed in a slow way to overcome the defects formed in the first stage. This stage was time-consuming. Approximately, the time of the first stage can be regarded as the time of the phase separation.

In order to discuss the influence of the temperature on the time evolution of the phase separation, the three pluronic

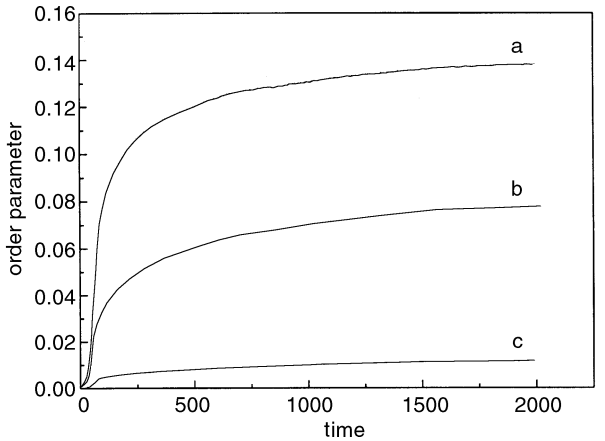

Fig. 5 Time evolution of the dimensionless order parameter P: the labels a, b and c refer to beads E, P and S, respectively.

Table 4 The time for phase separation

	Time/μs		
Temperature/K	L62	L64	P105
298	10	3.5	2.0
323	15	4.3	2.6
373	30	5.0	4.3

water mixtures have been simulated at three different temperatures: 298 K, 323 K, 373 K. Table 4 shows the simulation results.

The simulation results show that, when the temperature increases, the phase separation process becomes slow. The effects of temperature on the phase separation process can be understood as that the hydrophobicity of the polymer is enhanced when the temperature increases. The interaction between the copolymer and the water solvent takes a longer time and the periodicity of the morphology increases.

Conclusion

The Mesodyn 'equivalent chain' method was successfully used to simulate pluronic water mixtures and to describe the kinetic process. The simulation results show that with the same volume concentration of the polymer (0.50), the L62, L64 and P105 solutions formed gel, transition and micelle morphology respectively. This is in agreement with experiment.[18]

The influence of the temperature on the time evolution of the phase separation and the phase morphology is discussed. The Fourier transform result indicates that when the temperature increases, the frequency increases too. This result is the same as Alexandridis's work.[18] Their work shows that an increase of the temperature results in a decrease in the interfacial area and an increase in the periodicity of the L62 and L64 lamellae. Brown's experimental work[19] shows a similar result that the apparent micellar radius decreases with increasing temperature. The simulation result of the three polymer solutions indicates that with temperature increase, the phase separation process becomes slow. The effects of temperature on the phase separation process can be understood as that the hydrophobicity of the polymer is enhanced when the temperature increases. The interaction between the copolymer and the water solvent takes a longer time and the periodicity of the morphology increases.

Acknowledgement

This project is supported by NCSF 29992590-2.

References

1 Z. Tuzar and P. Kratochvil, *Adv. Colloid Interface Sci.*, 1976, **6**, 201.
2 Z. Zhou and B. Chu, *Macromolecules*, 1987, **20**, 309.
3 Z. Zhou and B. Chu, *J. Colloid Interface Sci.*, 1998, **126**, 171.
4 W. Brown, K. Schillen, M. Almgren, S. Hvidt and P. Bahadur, *J. Phys. Chem.*, 1991, **95**, 1850.
5 G. Wanka, H. Hoffmann and W. Ulbricht, *Colloid Polym. Sci.*, 1990, **268**, 101.
6 T. Valls and J. E. Farrell, *Phys. Rev.*, 1993, **E47**, R36.
7 T. Kawakatsu, K. Kawasaki, M. Furusaka, H. Okabayashi and T. Kanaya, *J. Chem. Phys.*, 1993, **99**, 8200.
8 A. Shinozaki and Y. Oono, *Phys. Rev.*, 1993, **E48**, 2622.
9 M. C. Cross and P. C. Hohenberg, *Rev. Mod. Phys.*, 1993, **65**, 851.
10 B. Schmittmann and R. K. P. Zia, in *Phase Transitions and Critical Phenomena*, ed. C. Domb and J. Lebowitz, Academic Press, London, 1994.
11 G. N. Malcolm and J. S. Rowlinson, *Trans. Faraday Soc.*, 1957, **53**, 921.
12 M. N. Barber and B. W. Ninham, *Random and Restricted Walks*, Gordon and Breach, New York, 1970.
13 A. Abe and J. E. Mark, *J. Am. Chem. Soc.*, 1976, **98**, 6468.
14 A. Abe, T. Hirano and T. Tsuruta, *Macromolecules*, 1979, **12**(6), 1092.
15 J. G. E. M. Fraaije and B. A. C. Van Vlimmeren, *J. Chem. Phys.*, 1997, **106**(10), 4260.
16 N. M. Maurits and B. A. C. Van Vlimmeren, *Phys. Rev. E*, 1997, **56**(1), 816.
17 B. A. C. Van Vlimmeren and J. G. E. M. Fraaije, *Comput. Phys. Commun.*, 1996, **99**, 21.
18 P. Alexandridis, D. Zhou and A. Khan, *Langmuir*, 1996, **12**, 2690.
19 W. Brown, K. Schillen and S. Hvidt, *J. Phys. Chem.*, 1992, **96**, 6038.
20 Z. Zhou and B. Chu, *J. Colloid Interface Sci.*, 1988, **126**, 171.